Biochemical and Biophysical Research Communications 415 (2011) 82–87

Contents lists available at SciVerse ScienceDirect

Biochemical and Biophysical Research Communications

journal homepage: www.elsevier.com/locate/ybbrc

Crystal structure of *Campylobacter jejuni* ChuZ: A split-barrel family heme oxygenase with a novel heme-binding mode

Rui Zhang [a], Jinyong Zhang [a], Gang Guo [a], Xuhu Mao [a], Wende Tong [a], Ying Zhang [b], Da-Cheng Wang [b], Yonglin Hu [b,*], Quanming Zou [a,*]

[a] Dept. of Clinical Microbiology and Immunology, Third Military Medical University, Chongqing 400038, People's Republic of China
[b] National Laboratory of Biomacromolecules, Institute of Biophysics, Chinese Academy of Sciences, 15 Datun Road, Beijing 100101, People's Republic of China

ARTICLE INFO

Article history:
Received 16 September 2011
Available online 12 October 2011

Keywords:
ChuZ
Heme oxygenase
Campylobacter jejuni
Crystal structure
Bacterial iron acquisition

ABSTRACT

The heme oxygenase ChuZ is part of the iron acquisition mechanism of *Campylobacter jejuni*, a major pathogen causing enteritis in humans. ChuZ is required for *C. jejuni* to use heme as the sole iron source. The crystal structure of ChuZ was resolved at 2.5 Å, and it was revealed to be a homodimer with a split-barrel fold. One heme-binding site was at the dimer interface and another novel heme-binding site was found on the protein surface. Heme was bound in this site by four histidine side-chains through hydrophobic interactions. Based on stoichiometry studies and comparisons with other proteins, the possibility that similar heme-binding site exists in homologous proteins and its possible functions are discussed. The structural and mutagenesis analyses reported here establish ChuZ and ChuZ homologs as a new bacterial heme oxygenase family apart from the canonical and IsdG/I families. Our studies provide insight into the enzymatic mechanisms and structure–function relationship of ChuZ.

1. Introduction

Iron is an essential nutrient that is required for nearly all forms of life. It is incorporated, either in free forms or as part of an iron-sulfur cluster and heme, into proteins involved in many important biological processes, such as oxygen or electron transport and redox reactions. For pathogenic bacteria that invade animal hosts, iron acquisition is of paramount importance because free iron is not biologically available [1]. Host cells sequester iron into porphyrins and carrier molecules, such as transferrin and ferritin, to minimize the damage caused by ferric iron (Fe^{2+}) via Haber-Weiss–Fenton reactions [2] and to restrict microbe growth [3]. Consequently, the iron acquisition systems of bacteria play important roles in their survival, virulence, and pathogenicity in animal hosts. Because of their abundance in animal hosts, hemoproteins are important, sometimes preferred, iron sources for pathogenic bacteria [4]. Bacteria have developed mechanisms to capture hemes and transport them into the cells. Once inside the bacteria, the hemes are either stripped of their iron atoms, leaving intact porphyrin rings, or they are degraded by heme oxygenases (HOs, E.C. 1.14.99.3) to release free iron.

HOs are mono-oxygenases that catalyze the oxidative cleavage of porphyrin rings to produce free iron, biliverdin, and carbon monoxide. Mammalian HOs have been extensively studied, but bacterial HOs have only recently been identified [5]. Most bacterial HOs have homologous sequences and similar structures with mammalian HOs. They are all-α-helical monomers with the hemes sandwiched between two α-helices. In recent years, a new family of bacterial HOs (IsdG/I) has been identified in the bacterial pathogens *Staphylococcus aureus* and *Bacillus anthracis* [6]. These HOs are composed of α/β-structures with ferredoxin-like folds [7]. We have recently identified a novel bacterial HO family that is distinct from all of the other characterized HOs with a split-barrel fold, based on the three-dimensional structure of *Helicobacter pylori* HugZ [8].

Here, we report the crystal structure of ChuZ, an HO from *Campylobacter jejuni*, complexed with hemin at 2.5 Å resolution. The gram-negative, micro-aerophilic bacterium *C. jejuni* is found in the gut of a wide range of food-supply animals and avian species. It is a major cause of acute gastroenteritis. Previous *C. jejuni* infection is also implicated in the development of serious immune-mediated neurological conditions known as Guillain-Barré and Miller-Fischer syndromes. Like other pathogenic bacteria, *C. jejuni* has an absolute requirement for iron, and it has numerous transport systems for capturing ferrous and ferric (Fe^{3+}) cations and heme [9]. Among them are an iron- and Fur-regulated gene cluster that encodes an ABC-type hemin transport system and ChuZ, which enables the bacterium to utilize hemin as the sole iron source [10]. ChuZ is a 251 amino-acid residue protein. Genotyping experiments revealed that it is highly conserved in 32 clinical isolates. Mutation of ChuZ abolishes the ability of *C. jejuni* to use

* Corresponding authors. Fax: +86 0 2368752315.
E-mail addresses: yonglin@ibp.ac.cn (Y. Hu), qmzou@mail.tmmu.com.cn (Q. Zou).

0006-291X/$ - see front matter © 2011 Published by Elsevier Inc.
doi:10.1016/j.bbrc.2011.10.016

hemin or hemoglobin as sources of iron [10,11], indicating the important role played by ChuZ in *C. jejuni* iron acquisition.

Based on structural and biochemical studies on ChuZ and several functionally relevant mutants, this work demonstrates that ChuZ is a new member of the split-barrel HO family. Although the structure of ChuZ and its interactions with heme are highly conserved with respect to those of *H. pylori* HugZ, a novel heme-binding site on the surface of ChuZ, which was not observed in HugZ, points to the possibility that in addition to its role as an HO, ChuZ may participate in heme accumulation. These studies greatly improve our understanding of this new bacterial HO family.

2. Materials and methods

2.1. Protein purification and crystallization

The purification and crystallization of ChuZ have been previously reported [12]. ChuZ has a strong intrinsic affinity toward nickel nitriloacetic (Ni–NTA) resin, and this affinity was utilized for purification. Briefly, a pET22b plasmid containing the *chuZ* gene was transformed into *Escherichia coli* BL21 (DE3) competent cells. These cells were grown in LB medium at 310 K until the A_{600} reached 0.6. Isopropyl-β-D-thiogalactoside was then added to a final concentration of 10 μM to induce protein expression. After growth at 295 K for 12 h, the cells were harvested by centrifugation, washed, and resuspended in a solution containing 50 mM phosphate pH 8.0, 300 mM NaCl (Solution A) supplemented with 10 mM imidazole; the bacteria were then lysed by ultrasonication on an ice bath. The lysate was cleared by centrifugation and filtration and loaded onto a Ni–NTA resin column (Novagen). The column was extensively washed with Solution A, which contained 20 mM imidazole, and ChuZ was eluted with Solution A supplemented with 100 mM imidazole. The sample was further purified by chromatography using a HiLoad 16/60 Superdex 200 gel filtration column (GE Healthcare) and then eluted in 20 mM Tris–HCl pH 8.0, 100 mM NaCl.

To reconstitute ChuZ with hemin, a 5 mM hemin solution in DMSO was added drop-wise into a ChuZ solution until the molar ratio of hemin:ChuZ reached 2:1. Then, a 0.5 M azide solution was added to a final concentration of 5 mM. The sample was incubated at 277 K overnight with gentle shaking. Excess hemin was removed by using a HiLoad 16/60 Superdex 200 gel filtration column (GE Healthcare). The ChuZ–hemin complex was eluted with a 20 mM Tris–HCl pH 8.0 buffer containing 5 mM sodium azide. The solution was concentrated for crystallization using ultrafiltration. Crystals of the ChuZ–hemin complex were obtained using the microbatch method by mixing 1 μl of 170 mg/ml ChuZ–hemin solution and 1 μl of a reservoir solution consisting of 0.1 M MES, 24% PEG400 (v/v), and 0.1 M imidazole pH 6.5.

The R166A mutant of ChuZ was purified using the same protocol as that of the wild-type ChuZ. The H9A/H14A double and H9A/H14A/R166A triple mutants had lower affinities for Ni–NTA resin. These two mutant proteins were loaded onto Ni–NTA columns in the presence of 5 mM imidazole, washed with a solution containing 10 mM imidazole, and eluted with the same elution solution as wild-type ChuZ. All of the mutant proteins were reconstituted with hemin as described above for wild-type ChuZ.

2.2. Data collection and structure determination

A diffraction dataset to 2.5 Å resolution was collected at Beam Line 17U of the Shanghai Synchrotron Radiation Facilities, Shanghai, China, as previously described [12]. The crystal structure was solved by the molecular replacement method with the program PHASER [13], using the structure of HugZ (PDB accession code 3GAS) as the search model. There was one ChuZ–hemin complex in the asymmetric unit. Structural refinement was performed using the PHENIX package [14]. Manual rebuilding of the model was performed using the program COOT [15].

Iterative cycles of refinement and manual model rebuilding were performed until the R_{work} and R_{free} were satisfactory. The final model contains residues 2–250. Residues 33 and 49–51 are missing because of poor density in these regions. The model is of good quality because 84.5% of the residues are located in the most favored regions of the Ramachandran plot and none are located in the disallowed regions, as calculated with the program PROCHECK [13]. The statistics for data collection and structural refinement are summarized in Table 1.

2.3. Enzymatic activity assays

The enzymatic activities of ChuZ and the ChuZ mutants were assayed by spectroscopic methods [16]. Briefly, 10 μM of protein and heme were added into 1 ml of a reaction solution of 20 mM Tris–HCl, pH 7.6, 150 mM NaCl. The solution was incubated at 298 K until the absorption at 410 nm stabilized. Then, 20 μl of 1 M L-ascorbic acid was added to start the reaction. The absorption was recorded at 2-min intervals for 40 min from 340 and 800 nm. All measurements were made at 298 K with a circulating water bath using a Hitachi U-2010 Spectrophotometer.

2.4. Hemin-binding assays using spectroscopic methods

The stoichiometry of ChuZ–hemin binding was assayed by spectroscopic methods. For the titration experiments, hemin was dissolved in DMSO at a concentration of 5 mM and diluted with 50 mM Tris–HCl pH 7.5 and 100 mM NaCl (Solution B) to 2.5 mM. Successive 1 μl aliquots of hemin were added into a sample cuvette containing 10 μM wild-type ChuZ or H9A/H14A double mutant in Solution B and a reference cuvette containing Solution B alone. After addition of each hemin aliquot, the samples were equilibrated for 10 min. before the UV spectra were recorded using a Unico 4802 UV/Vis Double Beam Spectrophotometer at 295 K.

For the dialysis experiments, aliquots of the hemin solution were added to 1 μM solutions of wild-type ChuZ and the H9A/H14A double mutant in Solution B to final concentrations of 1–10 μM. After incubating at 295 K for 30 min, the solutions were dialyzed overnight against Solution B at 277 K to remove excess hemin. The absorption spectra from 300 to 700 nm of the dialyzed solution were recorded using a Hitachi U-2010 Spectrophotometer at 295 K and adjusted according to the volume increase after dialysis.

Table 1
Data collection and refinement statistics.

Data collection	
Space group	$C222_1$
Unit cell dimensions (Å)	a = 106.47, b = 106.70, c = 52.46
Wavelength (Å)	0.9794
Resolution (Å)[a]	50–2.5 (2.54–2.5)
Unique reflections	10,407
Completeness (%)	97.3 (80.9)
Mean $I/\sigma(I)$	45.2 (3.8)
R_{merge} (%)[b]	5.5% (35.3%)
Refinement	
No. of residues	246
R_{work}/R_{free} (%)	21.2/27.2
RMSD bonds (Å)	0.010
RMSD angles (°)	1.061

[a] Values in parentheses are for the highest resolution shell.
[b] $R_{merge} = \sum_{hkl}\sum_i |I_i(hkl) - \langle I(hkl)\rangle| / \sum_{hkl}\sum_i I_i(hkl)$ where $I_i(hkl)$ is the ith intensity measurement of reflection hkl and $\langle I(hkl)\rangle$ its average.

2.5. Protein Data Bank accession number

The coordinates and structure factors of ChuZ have been deposited in the RCSB with accession code 3SWJ.

3. Results and discussion

3.1. Structure of the ChuZ–hemin complex with a unique split-barrel fold

The asymmetric unit of the crystal contains one molecule of the ChuZ–hemin complex. Because ChuZ and ChuZ–hemin behave as dimers in size-exclusion chromatography (data not shown) and previously characterized proteins with a split-barrel fold, including HugZ, are all dimeric, the ChuZ–hemin dimers are the functional units of this protein. The two monomers inside each dimer are related by a 2-fold crystallographic rotation axis that is coincident with *a* (Fig. 1A).

The structure of ChuZ consists of two distinct domains: residues 1–82 form the smaller N domain, while residues 83–251 form the larger C domain with a typical split-barrel fold. The two domains are relatively independent of each other and are connected by a flexible loop region (residues 78–86).

The N-domain is an α/β-type structure consisting of three α-helices (α1–α3) stacked against a three-stranded anti-parallel β-sheet (formed by β1–β3). The C-domain is a typical split-barrel fold, consisting of 8 β-strands (β4–β11) and 4 α-helices (α4–α7). The 8 β-strands are arranged anti-parallel to each other, with the first 6 strands, β4–β9, forming a β-barrel. Two short β-strands, β10 and β11, are located adjacent to the C-terminus of β9, the longest of the ChuZ β-strands. Parts of β7–β9 form a somewhat planar β-sheet with β10 and β11. One side of this β-sheet serves as the base of the heme-binding pocket, while the opposite side is stacked against helix α4. Helices α4 and α5 cap the two openings of the barrel, whereas α6 and α7 are adjacent to each other and stacked against the side of the β-barrel.

The ChuZ dimer is formed by stacking the β-barrels of two monomers at approximately 90°. A shape complementarity factor of 0.77, as calculated with the program SC [13], indicates a highly complementary surface at the dimer interface.

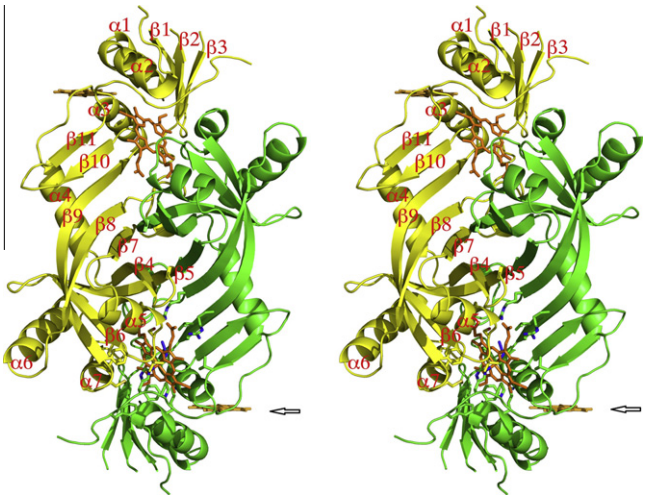

Fig. 1. The stereoview of the ChuZ–hemin complex. The two monomers of ChuZ are colored green and yellow and are related by a crystallographic 2-fold axis passing through the center of the figure, perpendicular to the plane. The heme moieties are shown as stick models. The arrow designates the heme bound on the surface of the protein.

3.2. Two distinct heme-binding sites of ChuZ

Two groups of density peaks, each clearly from a heme moiety, were observed on the σ_A-weighted difference map. When heme was modeled into each of these peaks (Fig. 2A and B), one of the heme moieties was located in the same binding site identified in HugZ, while the other moiety was on the surface of the molecule, bound by residues His9 and His14 from two symmetry-related ChuZ dimers.

3.2.1. The "canonical" heme-binding site

This binding site is located at the dimer interface, and it is bound by hydrogen bonds with its two carboxylate groups and extensive hydrophobic interactions between the porphyrin ring and residues from both monomers. In addition, the heme iron is coordinated by the Nτ atom of His245, which is located in a flexible C-terminal loop (Fig. 2C).

The heme-binding pocket has two distinct parts. At the end where the two carboxylate groups of the heme are located, the pocket is lined with hydrophilic side-chains, such as those of Lys166 and Lys219 from one monomer and Ser134 and His136 from the other. These side-chains form 7 direct or water-mediated hydrogen bonds with the heme carboxylate groups. The other part of the binding pocket, however, is lined with hydrophobic groups. These hydrophobic groups are provided by the side-chains of Val221, Phe224, Ala227, and Val238, and the main-chain of Gly225 on one side of the heme. The other side of the heme contains His245, and the side-chains of Pro244 and Phe247 as well as several residues from the other monomer, including Val133, Ile202, Met205, and Phe208, provide the hydrophobic groups (Fig. 2C). The only N-domain residues involved in heme-binding are the side-chains of Lys24 and Phe25, which bind the heme via hydrophobic interactions from the lateral direction.

After the reconstitution of ChuZ–hemin, azide was included in all of the solutions to prevent heme degradation and improve crystal quality. Thus, an azide molecule was found coordinating the iron as the sixth ligand with one of its terminal N atoms, designated N1. Because it coordinates the iron with its sp^2 hybrid orbital like O_2, the Fe–N–N angle is 121.5°, which is very close to the theoretical value of 120°. This bond angle was also very close to those observed in HugZ and in the canonical HO–hemin complexed with O_2, N_3^-, and NO [17–19].

3.2.2. A potential heme-binding site on protein surface

This heme-binding site is located at the interface between the two ChuZ dimers related by a crystallographic 2-fold axis, with the iron atom located on the axis at (½, −0.27, ¼) and the porphin ring perpendicular to the axis. With the 2-fold symmetry imposed on the asymmetric heme molecule, only the porphin ring and iron atom, which make up a unit with 2-fold symmetry, are visible. The substituent groups on the porphin ring are missing from the electron density map and are not included in the refined model (Fig. 2B).

The surface heme is bound to ChuZ by the side-chains of His9 and His14 from two neighboring ChuZ dimers through hydrophobic interactions with the porphin ring (Fig. 2D). Two structural features, the unfavorable bond angles and the long distances (larger than 4.4 Å) between the imidazole atoms and the iron, exclude the possibility of Fe–N bond formation. However, the closest distances between the imidazole atoms of His9 and His14 and the plane of the porphin ring are 3.05 and 3.11 Å, respectively. This indicates that strong interactions exist between the imidazole ring and the delocalized electron densities of the porphin ring. In relation to the heme, the imidazole planes of His9 and His14 are at angles of 85° and 35°, respectively. Residues from α3, although close, do not interact with the heme (Fig. 2C).

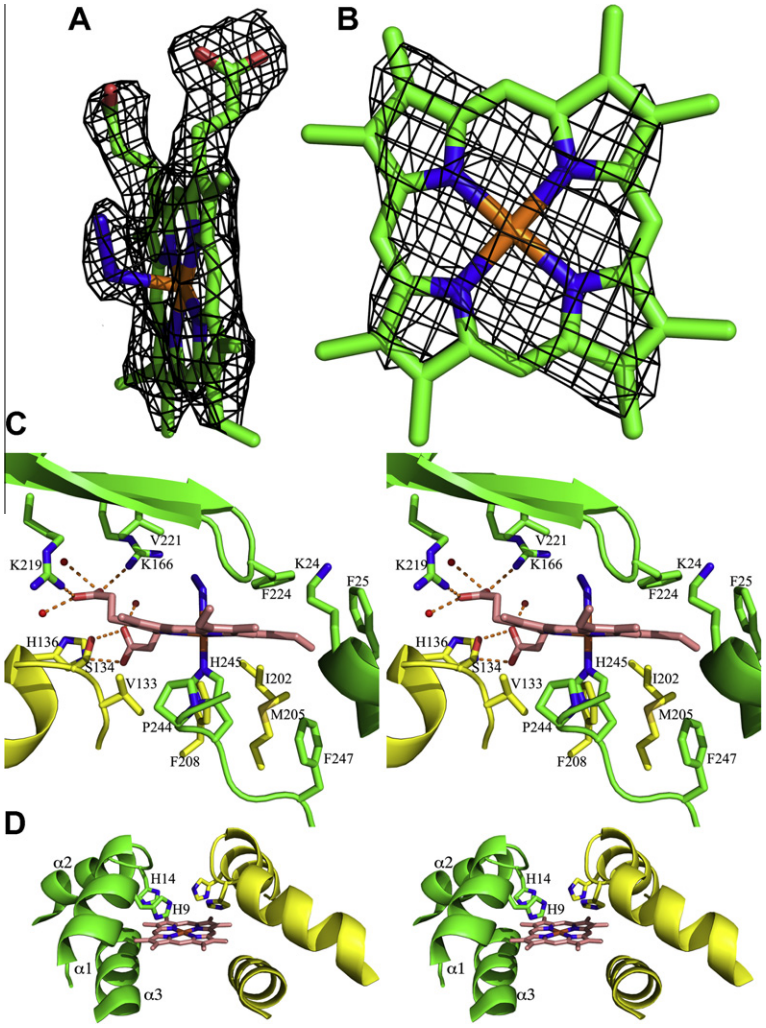

Fig. 2. Heme-binding sites and ChuZ–heme interactions. (A) The σ_A-weighted simulated annealing $2F_o - F_c$ omit map around the heme and azide moieties at the heme-binding pocket, contoured at 1σ. (B) The σ_A-weighted simulated annealing $2F_o - F_c$ omit map around the "extra" heme, contoured at 1σ. (C) Stereoview of the ChuZ–heme interactions. (D) Stereoview of the interactions between ChuZ and the "extra" heme.

To verify the existence of this surface heme-binding site, we measured the stoichiometry of heme binding by wild-type ChuZ and the H9A/H14A mutant by spectroscopic methods. In the first experiment, ChuZ samples were titrated with hemin solution and the results clearly show a heme-binding stoichiometry of 1.5 for wild-type ChuZ and 1 for the H9A/H14A mutant. In the second example, samples of protein–heme complexes were first prepared with different heme:protein molar ratios. The excess heme was then removed by extensive dialysis at 277 K and the absorption spectra were recorded between 340 and 500 nm. For the wild-type protein, the absorption at 410 nm, the Soret peak of ChuZ–heme complexes, continued to increase until the heme:protein molar ratio reached 1.5. Conversely, for the H9A/H14A double mutant, the absorption at 410 nm did not significantly change after the heme:protein molar ratio reached 1.0 (Fig. 3). These results correlated very well with the observation that 1 heme molecule is bound on the surface of the ChuZ dimer in addition to 1 heme per ChuZ monomer inside the binding pocket. The results also suggest that mutation of His9 and His14 removes the surface heme-binding site and resulted in a 1:1 ChuZ–hemin binding stoichiometry.

Similar heme-binding site might also exist in homologous HOs. During our previous work on *H. pylori* HugZ, we observed that the protein could bind significantly more hemin than 1:1 M ratio (data not shown). This observation correlates well with the fact that both His9 and His14 are conserved in HugZ.

3.2.3. Possible function of the surface heme-binding site

The heme-binding site on the ChuZ surface is unique in two aspects; it is formed exclusively by non-covalent bond hydrophobic interactions, and the heme is highly exposed. This unique protein–heme interaction is reminiscent of the Cu, Zn superoxide dismutase (HdSOD) from *Haemophilus ducreyi* [20] in which a heme is bound on the protein surface at the interface between two HdSOD monomers. The heme moiety is completely exposed to the environment on HdSOD, although a histidine side-chain coordinates the bound heme on HdSOD. This heme-binding site was proposed to participate in the accumulation of hemes in *H. ducreyi* cells. Many bacterial proteins were found to be able to accumulate hemes such as HdSOD, and these proteins contribute to the suppression of heme toxicity and the pathogenicity of the bacteria [21].

The fact that the heme at the surface binding site of ChuZ was retained after extensive dialysis in stoichiometry studies and after lengthy purification processes prior to crystallization suggests that it may not be a mere crystal packing artifact. It is also noteworthy that similar heme-binding site might also exist in *H. pylori* HugZ, a homologous HO. We therefore propose that this heme-binding site

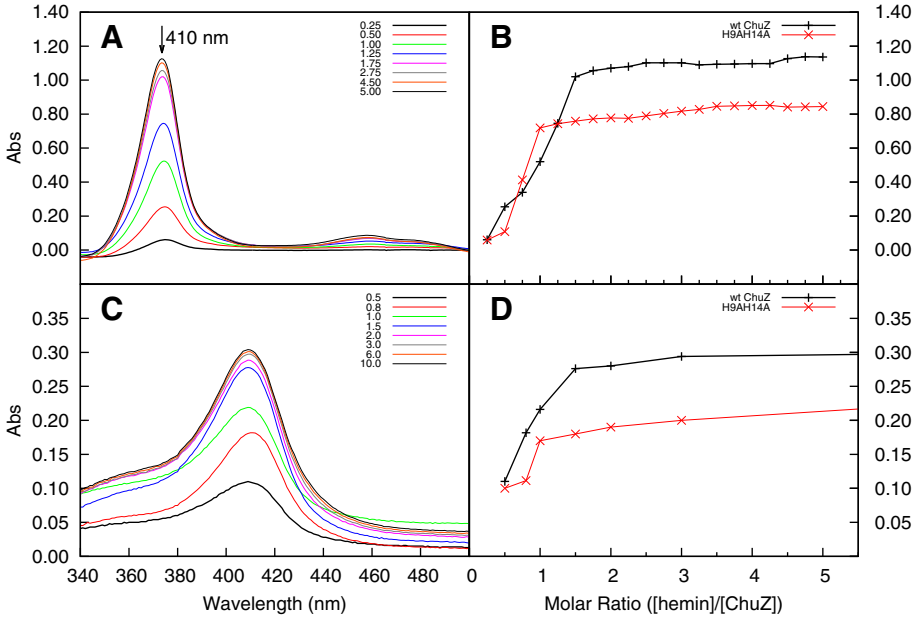

Fig. 3. Heme-binding stoichiometry assays. (A) Difference UV spectra of heme titration of ChuZ at selected heme:protein molar ratios. (B) Change in absorbance at 410 nm versus heme:protein molar ratio. The heme-binding of wild-type and H9A/H14A mutant ChuZ are saturated at heme:protein molar ratio of 1.5 and 1, respectively. (C) UV spectra of ChuZ–heme complex at different heme:protein molar ratio after dialysis. (D) The wild-type and H9A/H14A mutant of ChuZ retain 1.5 and 1 heme per protein, respectively.

might be functional and heme accumulation might be one of the possible roles played by this site.

To further verify the roles played by His9 and His14 in the surface heme-binding site, we purified and crystallized a H9A/H14A double mutant complexed with heme. However, the crystal could not diffract to a resolution better than 3.3 Å despite extensive searches for crystallization conditions. The mutant crystal has a different space group ($P6_522$, with $a = b = 51.76$ Å and $c = 383.29$ Å) than the wild-type ChuZ crystal. Preliminary molecular replacement studies showed that the molecular packing around residues His9 and His14 is different than that in ChuZ, but structural refinement at this resolution did not progress very smoothly. Efforts to obtain crystals of higher quality are under way.

3.3. Structural conservation of ChuZ and mechanistic implications

The structure of ChuZ is similar to that of HugZ, with a root-mean-square deviation (RMSD) of 1.2 Å for 236 Cα atoms from both domains. The structural similarity is much higher for the C-domain, with an RMSD of 0.85 Å for 163 Cα atoms. The β-barrels

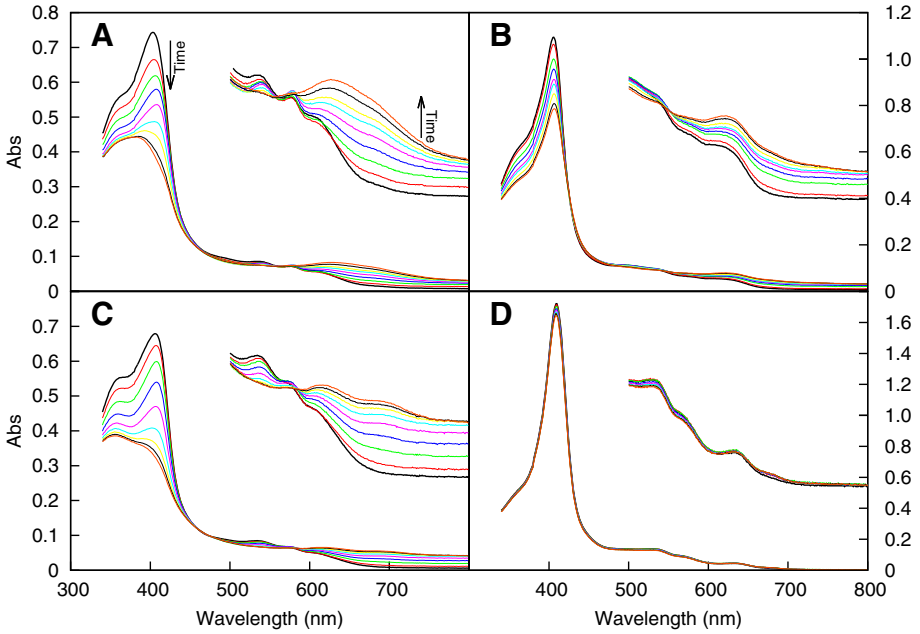

Fig. 4. Enzymatic activity assays of wild-type ChuZ (A), the R166A mutant (B), the H9A/H14A double mutant (C), and the H9A/H14A/R166A triple mutant (D). The spectra were recorded at 2 min. intervals. The decrease of the peak at 410 nm indicated the degradation of heme, while the increase of the absorption in the 500–800 nm range indicated the production of biliverdin. The spectra between 500 and 800 nm are magnified 5× in the insets.

of these two proteins are especially well conserved; a small RMSD of 0.34 Å was observed for the superposition of 53 Cα atoms from 6 β-strands of the β-barrels, highlighting the highly rigid nature of the barrel structure.

Almost all of the residues lining the heme-binding pockets of ChuZ and HugZ are conserved between the two proteins. Consequently, the heme-binding sites and the conformations of the bound heme are completely conserved. Residue Arg166, which was identified as the residue essential for the enzymatic mechanisms of HugZ [8], is conserved in ChuZ, and its side-chain occupies the same position as in HugZ. However, enzymatic assays showed that the R166A mutant has diminished but still detectable heme-degrading activities (Fig. 4B). We propose that this phenomenon might be the result of the degradation of the surface-bound heme by non-enzymatic oxidations. Indeed, the H9A/H14A/R166A triple mutant was completely inactive (Fig. 4D).

It is interesting to note that the azide molecule at the first heme-binding site adopted the same conformation as in the HugZ structure; i.e., it bisects pyrrole IV of the porphin, and the N3 atom of this molecule is equidistant to α-*meso* and β-*meso* carbon atoms at 4.2 Å. In the structures of canonical HOs complexed with O_2 (or O_2 analogs N_3^- and NO), the terminal atoms of the bound O_2/N_3^-/NO was always near α-*meso* carbons, and this was proposed to be the structural basis of the α-*meso* regiospecificities of the ring-opening reactions of these enzymes in degrading hemes [17,18]. It was also proposed that the unique δ-*meso* regiospecificity of HugZ was determined by the conformation of the azide molecule in the HugZ–heme–azide complex structure [8]; therefore, it is likely that ChuZ has an α- and/or δ-*meso* regiospecificity because the azide molecule has the same conformation as that in HugZ.

Significant structural changes between these two proteins mostly occur in the loop regions, i.e., the loop regions between β5/β6 and β10/β11 and the C-terminal loop region (Gly239–His251). While Pro244 and His245 both participate in heme-binding and superimpose with their counterparts from HugZ, the rest of the C-terminal loop differs remarkably between ChuZ and HugZ, indicating that with the exception of these two residues, this region is not essential for the enzymatic mechanisms of ChuZ.

The field of iron acquisition by pathogenic bacteria has witnessed rapid progress in the past few years, especially for the proteins involved in heme acquisition, transportation, and degradation. These proteins have attracted great interest as promising targets for the development of novel anti-bacterial drugs because the competition for iron, especially from heme sources, is one of the most important host–pathogen interactions during bacterial infections. The identification and characterization of two bacterial HO families, the canonical HO family homologous to human HO-1 and the IsdG/I family, greatly improved our understanding of bacterial iron acquisition from heme sources. Current work, together with previous biochemical characterizations of ChuZ and HugZ and the structural characterization of HugZ, firmly establishes a third bacterial HO family in addition to the canonical and IsdG/I families. The HO family with a split-barrel fold has several distinct features. They have highly conserved three-dimensional structures as indicated by the surprisingly small RMSDs between the Cα atoms from the β-barrels of ChuZ and HugZ; they have a very flexible loop as part of their heme-binding pockets, in contrast to the rigid heme-binding pockets of other HO families; and in addition to their "canonical" heme-binding site, they might have additional heme-binding sites on their surfaces. These features may provide us with new strategies to disrupt the iron acquisition pathways of pathogenic bacteria in our fight against bacterial infections.

Acknowledgments

We thank Z. Li and C. Li in the Department of Neurology at the Second Hospital of Hebei Medical University for providing the genome of *Campylobacter jejuni* NCTC 11168. We thank the staff at Beam Line 17U, Shanghai Synchrotron Radiation Facility, for their help with data collection. We thank Dr. Zheng Fan of the Institute of Microbiology, Chinese Academy of Sciences for technical assistance. This project was supported by National 973 Programs (2011CB911103, 2011CB910304, 2009CB522606) and the National Natural Science Foundation of China Grant 81072493.

References

[1] C. Wandersman, P. Delepelaire, Bacterial iron sources: from siderophores to hemophores, Ann. Rev. Microbiol. 58 (2004) 611–647.
[2] W.H. Koppenol, The Haber-Weiss cycle – 70 years later, Redox Rep. 6 (2001) 229–234.
[3] T. Ganz, Iron in innate immunity: starve the invaders, Curr. Opin. Immunol. (2009) 63–67.
[4] E.P. Skaar, M. Humayun, T. Bae, K.L. DeBord, O. Schneewind, Iron-source preference of *Staphylococcus aureus* infections, Science 305 (2004) 1626–1628.
[5] N. Frankenberg-Dinkel, Bacterial heme oxygenases, Antioxid. Redox Signaling 6 (2004) 825–834.
[6] E.P. Skaar, A.H. Gaspar, O. Schneewind, *Bacillus anthracis* IsdG, a heme-degrading monooxygenase, J. Bacteriol. 188 (2006) 1071–1080.
[7] W.C. Lee, M.L. Reniere, E.P. Skaar, M.E.P. Murphy, Ruffling of metalloporphyrins bound to IsdG and IsdI, two heme-degrading enzymes in *Staphylococcus aureus*, J. Biol. Chem. 283 (2008) 30957–30963.
[8] Y. Hu, F. Jiang, Y. Guo, X. Shen, Y. Zhang, R. Zhang, G. Guo, X. Mao, Q. Zou, D.C. Wang, Crystal structure of HugZ, a novel heme oxygenase from *Helicobacter pylori*, J. Biol. Chem. 286 (2011) 1537–1544.
[9] A.H. van Vliet, J.M. Ketley, S.F. Park, C.W. Penn, The role of iron in *Campylobacter* gene regulation, metabolism and oxidative stress defense, FEMS Microbiol. Rev. 26 (2002) 173–186.
[10] K.A. Ridley, J.D. Rock, Y. Li, J.M. Ketley, Heme utilization in *Campylobacter jejuni*, J. Bacteriol. 188 (2006) 7862–7875.
[11] C.L. Pickett, T. Auffenberg, E.C. Pesci, V.L. Sheen, S.S. Jusuf, Iron acquisition and hemolysin production by *Campylobacter jejuni*, Infect. Immun. 60 (1992) 3872–3877.
[12] R. Zhang, J. Zhang, H. Ding, D. Lu, Y. Hu, Q. Zou, D.C. Wang, Crystallization and preliminary crystallographic studies on Campylobacter jejuni ChuZ, member of a novel heme oxygenase family, Acta Crystallogr., Sect. F, 67 (2011) 1228–1230.
[13] Collaborative Computational Project Number 4, The CCP4 suite: programs for protein crystallography, Acta Crystallogr., Sect. D: Biol. Crystallogr. 50 (1994) 760–763.
[14] P.D. Adams, P.V. Afonine, G. Bunkoczi, V.B. Chen, I.W. Davis, N. Echols, J.J. Headd, L.W. Hung, G.J. Kapral, R.W. Grosse-Kunstleve, A.J. McCoy, N.W. Moriarty, R. Oeffner, R.J. Read, D.C. Richardson, J.S. Richardson, T.C. Terwilliger, P.H. Zwart, PHENIX: a comprehensive Python-based system for macromolecular structure solution, Acta Crystallogr., Sect. D: Biol. Crystallogr. 66 (2010) 213–221.
[15] P. Emsley, K. Cowtan, Coot: model-building tools for molecular graphics, Acta Crystallogr., Sect. D: Biol. Crystallogr. 60 (2004) 2126–2132.
[16] Y. Guo, G. Guo, X.H. Mao, W.J. Zhang, J. Xiao, W.D. Tong, T. Liu, B. Xiao, X.F. Liu, Y.J. Feng, Q.M. Zou, Functional identification of HugZ, a heme oxygenase from *Helicobacter pylori*, BMC Microbiol. 8 (2008) 226.
[17] S. Takahashi, K. Ishikawa, N. Takeuchi, M. Ikedasaito, T. Yoshida, D.L. Rousseau, Oxygen-bound heme–heme oxygenase complex – evidence for a highly bent structure of the coordinated oxygen, J. Am. Chem. Soc. 117 (1995) 6002–6006.
[18] M. Sugishima, H. Sakamoto, Y. Higashimoto, Y. Omata, S. Hayashi, M. Noguchi, K. Fukuyama, Crystal structure of rat heme oxygenase-1 in complex with heme bound to azide – implication for regiospecific hydroxylation of heme at the α-*meso* carbon, J. Biol. Chem. 277 (2002) 45086–45090.
[19] M. Sugishima, H. Sakamoto, M. Noguchi, K. Fukuyama, Crystal structures of ferrous and CO-, CN-, and NO-bound forms of rat heme oxygenase-1 (HO-1) in complex with heme: structural implications for discrimination between CO and O_2 in HO-1, Biochemistry 42 (2003) 9898–9905.
[20] I. Toro, C. Petrutz, F. Pacello, M. D'Orazio, A. Battistoni, K. Djinovic-Carugo, Structural basis of heme binding in the Cu, Zn superoxide dismutase from *Haemophilus ducreyi*, J. Mol. Biol. 386 (2009) 406–418.
[21] L.L. Anzaldi, E.P. Skaar, Overcoming the heme paradox: heme toxicity and tolerance in bacterial pathogens, Infect. Immun. 78 (2010) 4977–4989.